Electronic Supplementary Material (ESI) for ChemComm.

Electronic Supplementary Information

Mechanistic Investigation of Electrocatalytic Reductive Amination at Copper Electrode

Taemin Kim [a], Dong Il Park [a], Sojin Kim [a], Dibya Yadav [a], Sugyeong Hong [b], Sun Hee Kim [b], Hyo Jae Yoon[*a] and Kyoungsuk Jin[*a]

a: Department of Chemistry, Korea University, Seoul, 02841, Republic of Korea.

* E-mail: hyoon@korea.ac.kr, kysjin@korea.ac.kr

b: Western Seoul Center, Korea Basic Science Institute, and Department of Chemistry and Nano Science, Ewha Woman's University, Seoul, 120-140, Republic of Korea

Table of Contents

Experimental Procedures

A. Materials and Methods

A.1. Materials

Copper foil (0.127 mm thick, annealed, 99.9 %, Alfa aesar), Zinc foil (0.25 mm thick, 99.98 % metal basis, Alfa aesar), Platinum foil (0.02 mm thick, 99.95 %, Nilaco), Iron foil (0.127 mm thick, 99.5 % metal basis, Alfa aesar), Palladium foil (0.025 mm, 99.9 % metal basis, Alfa aesar), Nickel foil (0.1 mm thick, 99.5 % metal basis, Alfa aesar), disposable Aluminum foil (0.015 mm thick, Seongwoon), carbon paper (AV-carb MGL 190), Palladium on carbon (Pd/C, 5 wt%, matrix activated carbon support, Sigma), acetophenone(99 %, Sigma), methylamine solution(33 wt% in absolute ethanol, Sigma), dimethyl sulfoxide(DMSO, >99.0 %, TCI), tetrabutylammonium hexafluorophosphate($^{n}Bu_4PF_6$, >98.0 %, TCI), sodium perchlorate (NaClO4, 98.0 – 102.0 %, Alfa aesar), potassium hexafluorophosphate (KPF_6, 98%, Alfa aesar), anhydrous acetonitrile(ACN, 99.8+ %, Alfa aesar), anhydrous methanol(MeOH, 99.8 %, Acros), N,N-dimethylformamide (DMF, 99.8 %, Alfa aesar), tetrabutylammonium bromide ($^{n}Bu_4Br$, >99 %, Alfa aesar), acetic acid (CH_3COOH, 99.5 %, DAEJUNG), triethylamine(TEA, 99+ %, Alfa aesar), phenol(PhOH, 99+ %, Sigma), celite (Celite®535, Alfa aesar), dichloromethane (DCM, 99.5 %, SAMCHUN), n-hexane (95.0 %, DUKSAN), ethyl acetate (EA, 99.5 %, DUKSAN), DMSO-d_6(99.9 % D atom, Alfa aesar), chloroform-d ($CDCl_3$, 99.8 atom % D, Sigma), acetone (99.5 %, DAEJUNG), aniline (99+ %, Alfa aesar), (S)-(-)-N-Methyl-1-phenylethylamine (**1a**, >98.0 (GC)(T)%, TCI), N-phenylbenzylamine (**2a'**, 99 %, Alfa aesar), 4'-chloroacetophenone (97 %, Sigma), 4-acetylbenzonitrile (98+ %, Alfa aesar), 4'-nitroacetophenone (98%, Alfa aesar), 4'-Methoxyacetophenone (99%, Sigma), 4'-methylacetophenone (96 %, Alfa aesar), 4'-Fluoroacetophenone (99%, Sigma), 4'-(Trifluoromethyl)acetophenone (98+ %, Alfa aesar), Sodiumborohydride (97 %, DAEJUNG), isopropyl alcohol(99.5 %, DAEJUNG), silica plate (Sigma-Aldrich TLC plates, silica gel 60 matrices, Sigma). Molecular sieves(4 Å, 0.4-0.8 mm beads, Alfa aesar) were washed in acetone and dried at 400 ℃ for 2 hours using Muffle Furnace (digital muffle furnace FX-14, Daihan scientific)before being used. Water was purified using an Aqua MAX-Basic System (deionized water, the electrical resistivity of which is ~18.2 MΩ·cm)

A.2. Synthesis of Imines

The purity of imines was confirmed (>98%) before every use by gas chromatography-mass spectroscopy (GC-MS) mentioned in section **C.2.**

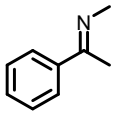

1(N-(1-phenylethylidene)methanamine): Prepared by adding 1.2 mL acetophenone (10 mmol) to 7 mL methylamine solution (ca. 50 mmol). The mixture was kept in r.t. for at least 24 hours in the presence of ca. 1.5g molecular sieves. The resulting imines were filtered with DCM using Celite and dried before use.

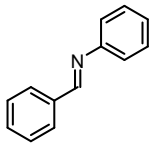

2(N-benzylideneaniline)**:** Prepared by adding 1 equivalent of the corresponding aniline to carbonyls in a 4 mL toluene solution. The mixture was heated to 60 – 70℃ for at least 48 hours for near quantitative yield. The resulting imines were filtered and dried before use.

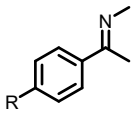

3(R = CN, 4-[1-(Methylimino)ethyl]benzonitrile), **4**(R = Me, *N*-[1-(4-Methylphenyl)ethylidene]methanamine), **5**(R = OMe, *N*-[1-(4-Methoxyphenyl)ethylidene]methanamine), **6**(R = F, [*N*(*E*)]-*N*-[1-(4-Fluorophenyl)ethylidene]methanamine), **7**(R = CF_3, [*N*(*E*)]-*N*-[1-[4-(Trifluoromethyl)phenyl]ethylidene]methanamine), **8**(R = NO_2, Methanamine, *N*-[1-(4-nitrophenyl)ethylidene]-, (*E*)-), **9**(R=Cl, *N*-[1-(4-Chlorophenyl)ethylidene]methanamine): Prepared by adding 2.5 mmol of the corresponding acetophenone derivatives to 3.5 mL methylamine solution (ca. 25 mmol). The mixture was kept in r.t. (3, 7, 8, 9) or heated (4, 5, 6) to 80℃ in the presence of ca. 1.5g molecular sieves for at least 24 hours. The resulting imines were filtered with DCM using Celite and dried before use.

A.3. Synthesis of Amines

Corresponding amines for **3** - **8** were prepared thermodynamically to obtain an external GC-MS calibration curve to quantify the electrochemical reductive amination (ERA) product of **3** - **8**.

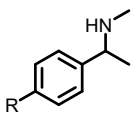

3a(R = CN, 4-[1-(Methylamino)ethyl]benzonitrile), **4a**(R = Me, *N*-Methyl-1-(4-methylphenyl)ethylamine), **5a**(R = OMe, 4-Methoxy-*N*,α-dimethylbenzenemethanamine), **6a**(R = F, 4-Fluoro-*N*,α-dimethylbenzenemethanamine), **7a**(R = CF_3, *N*,α-Dimethyl-4-(trifluoromethyl)benzenemethanamine), **8a**(R=NO_2, *N*,α-Dimethyl-4-nitrobenzenemethanamine): Followed the reported reductive amination protocols[1] using $NaBH_4$. 130 µmol imine was dissolved in 1.0 mL MeOH and 518 µmol of $NaBH_4$ was added at ambient conditions. After 12 hours of stirring, the reaction was quenched by adding brine, and the product was extracted with DCM and dried over the reduced pressure.

B. Electrochemical study

B.1. Electrode preparation

All metal foils except for Pt were washed with water and acetone, followed by 10 min sonication before use. Pt foil was treated with sonication in 1.0 M HCl and washed with water and acetone. Pd/C electrode prepared by the drop-casting method. Pd/C powder, distilled water, and IPA were mixed at the ratio of 1 mg: 10 µL: 15 µL to make catalyst ink and sonicated for 10 minutes. One side of carbon paper was drop-casted with 20 µL ink and dried in the oven for 1 minute. Then, the other side was drop-casted with the same amount of ink and dried in the oven for at least 30 minutes. All electrode materials were thoroughly dried before use.

B.2. Electrochemical methods

All electrochemical measurements were conducted using an undivided three-electrode system in a 2 mL sandwich-type cell. Cu foil and Zn foil were used as the working and counter electrodes, respectively, unless mentioned. The geometric surface area of the working electrode was 1.21 cm^2. An Ag/AgCl electrode (3.4 M KCl leak-free 2.0mm diameter Innovative Instruments) was used as the reference electrode and Al foil was used as the current collector. A magnetic spin bar (oval, 10 x 5 mm, SciLab) was placed into the cell and a magnetic stirrer (MS-12D Mini Digital Magnetic Stirrer, Daihan Scientific) was used for stirring during the electrolysis.

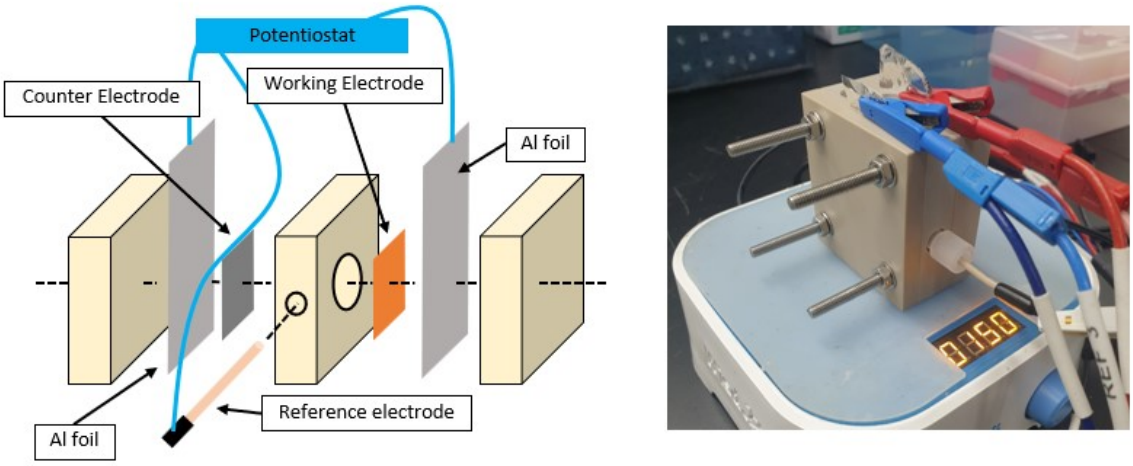

Figure S1. Description of electrochemical cell in the diagram (left) and picture (right).

As for the solvent, DMSO with 0.3 M $^nBu_4PF_6$ was used unless mentioned and molecular sieves were added to the solvent at least 30 minutes before the experiments to remove residual water. In each measurement, 1.8 mL of a solution containing substrates was added to the cell **(Figure S1)**. All electrochemical experiments were performed with a Biologic VSP3e potentiostat controlled via EC-Lab v11.36 software. All the potentials were manually 85% IR compensated based on the resistance value at open circuit potential (OCP) which was measured by EIS techniques. Cyclic voltammetry (CV) curves were recorded to investigate the electrochemical active behaviors. CV scans were initiated from the open-circuit potential, and four cycles (From OCP to -3.46 V vs Fc/Fc^+) were recorded successively at a scan rate of 50 mV/sec. The chronopotentiometry analysis (CP) was conducted at -1.65 mA/cm^2 until 8 C of charge was collected or chronoamperometry analysis (CA) was conducted at -2.86 V vs Fc/Fc^+ until 5 C of charge was collected to optimize the reactions. CA was conducted at -2.46 V vs Fc/Fc^+ to derive the kinetic isotope effect and effect of PhOH, and -2.86 V vs Fc/Fc^+ until 3 C of charge was collected to obtain electrokinetic data.

The detailed reaction conditions for **Figure 1a** were the same as the initial except for variables; Entry 1 - Cu/Pt, Entry 2, 3, and 4 - 100 mM $^nBu_4PF_6$ in ACN, MeOH, and DMF respectively, Entry 5,6, and 7 - 300 mM $NaClO_4$, KPF_6, and $^nBu_4Br$ respectively, Entry 8,9 - 50 mM CH_3COOH and TEA respectively, Entry 10 - -2.86 V vs. Fc/Fc^+ for 5 C passed.

C. Product analysis

C.1. NMR spectroscopy

^{1}H magnetic resonance (NMR) spectrum was recorded on a Bruker FT-NMR Advance-500 using $CDCl_3$ or DMSO-d6 as solvent.

C.1.1. NMR spectrum for amines

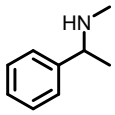

1a (N-methyl-N-(1-phenylethyl)amine): 34.7 C (2 F/mol) electric charge was applied in the optimized condition mentioned in Table 1 in three times. These samples were mixed and 1a isolated using thin-layer preparative chromatography using a silica plate with the mixture of hexane, ethyl acetate, and triethylamine (volume ratio was 5: 5: 1) as eluent. ^{1}H NMR (500 MHz, DMSO-d_6): δ=7.31-7.29 (m, 4H; Ar-H), 7.21-7.18 (m, 1H; Ar-H), 4.65 (s, 1H; NH), 3.53 (q, J=6.6 Hz, 1H; CH), 2.11 (s, 3H; CH_3), 1.21 (d, J=6.6, 3H; CH_3). Solvent residual peaks[2]: δ=8.06 (s, Chloroform), 5.73 (s, DCM), 4.02 (q, 2H; EA), 1.98 (s, 3H; EA), 1.17 (t, 3H; EA), 3.31 (br s, water), 2.54 (s, DMSO)

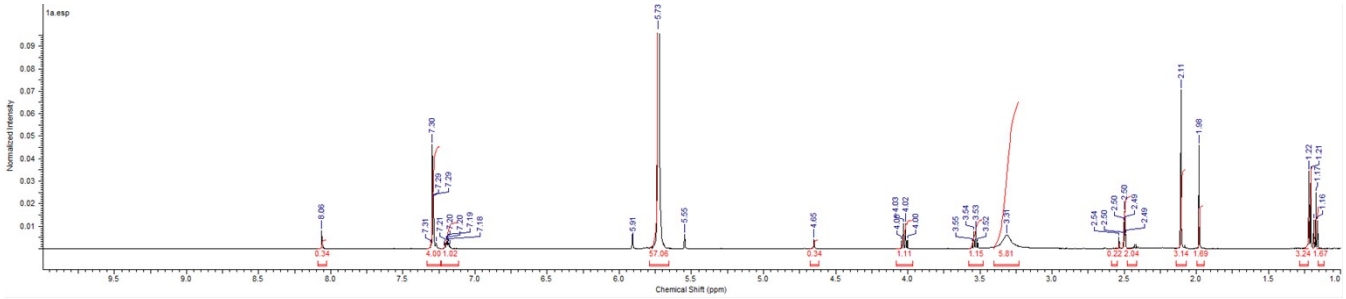

Figure S2. ^{1}H NMR spectrum of compound **1a** in DMSO-d_6, 500 MHz.

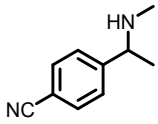

3a: Synthesized according to section **A.3.** ^{1}H NMR (500 MHz, CDCl3): δ= 7.60 (d, J=7.9 Hz, 2H; Ar-H), 7.42 (d, J=8.1 Hz, 2H; Ar-H), 3.68 (q, J=6.6 Hz, 1H; CH), 2.27 (s, 3H; CH_3), 1.32 (d, J=6.6 Hz, 3H; CH_3). Solvent residual peaks: 5.29 (s, DCM), 1.49 (br s, water), 1.24 (br s, H grease)

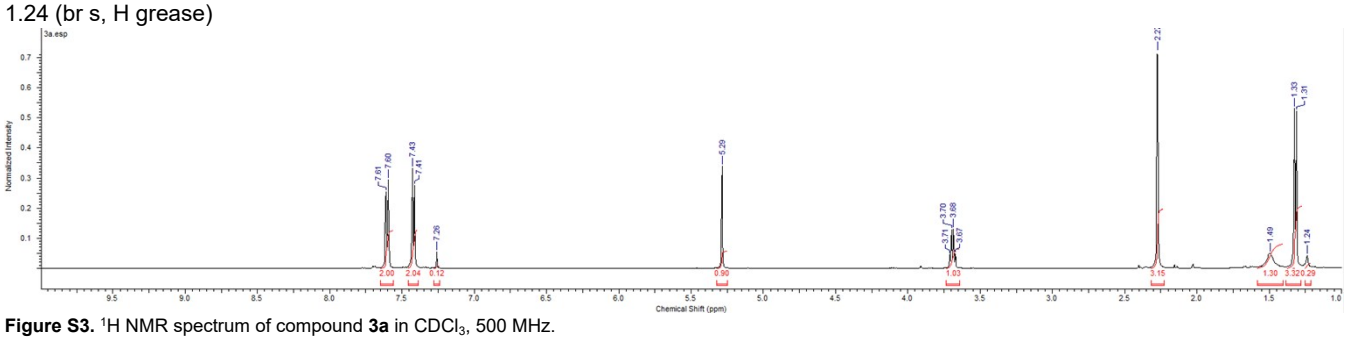

Figure S3. ^{1}H NMR spectrum of compound **3a** in $CDCl_3$, 500 MHz.

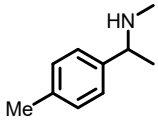

4a: Synthesized according to section **A.3.** ^{1}H NMR (500 MHz, $CDCl_3$): δ= 7.19-7.12 (m, 4H; Ar-H), 3.60 (q, J=6.4 Hz, 1H; CH), 2.33 (s, 3H; CH_3), 2.29 (s, 3H; CH_3), 1.33 (d, J=6.6 Hz, 3H; CH_3). Solvent residual peaks: 5.29 (s, DCM), 1.60 (br s, water), 1.25 (br s, H grease)

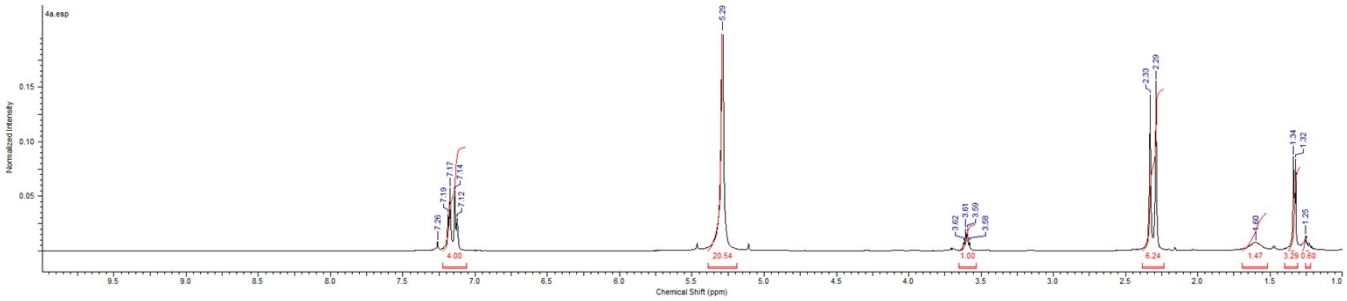

Figure S4. ^{1}H NMR spectrum of compound **4a** in $CDCl_3$, 500 MHz.

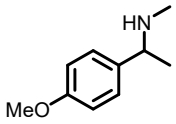

5a: Synthesized according to section **A.3.** ^{1}H NMR (500 MHz, $CDCl_3$): δ= 7.21 (d, J=8.5 Hz, 2H; Ar-H), 6.86 (d, J=8.5 Hz, 2H; Ar-H), 3.79 (s, 3H, CH_3), 3.59 (q, J=6.6 Hz, 1H; CH), 2.29 (s, 3H; CH_3), 1.32 (d, J=6.6 Hz, 3H; CH_3). Solvent residual peaks: 5.28 (s, DCM), 1.59 (br s, water), 1.25 (br s, H grease)

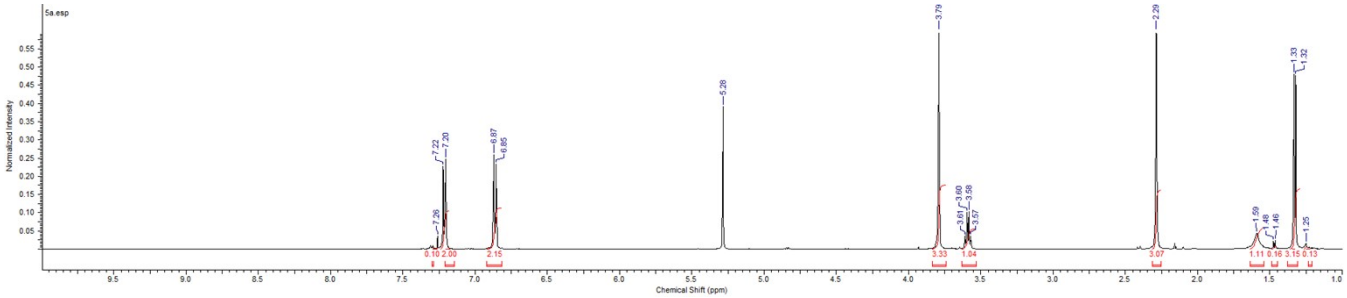

Figure S5. ^{1}H NMR spectrum of compound **5a** in $CDCl_3$, 500 MHz.

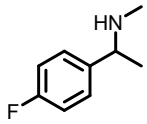

6a: Synthesized according to section **A.3.** ^{1}H NMR (500 MHz, $CDCl_3$): δ= 7.27-7.24 (m, 2H; Ar-H), 7.03-6.98 (m, 2H; Ar-H), 3.62 (q, J=6.6 Hz, 1H; CH), 2.28 (s, 3H; CH_3), 1.32 (d, J=6.6 Hz, 3H; CH_3). Solvent residual peaks: 5.28 (s, DCM), 1.75 (br s, water), 1.25 (br s, H grease)

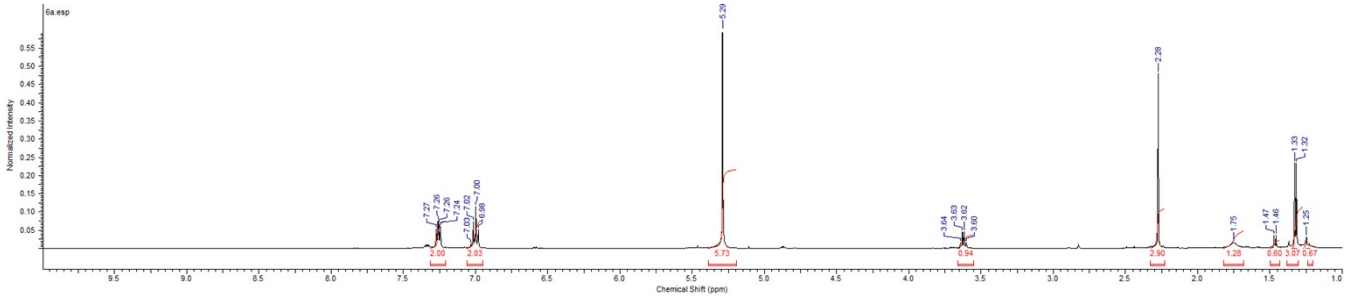

Figure S6. ^{1}H NMR spectrum of compound **6a** in $CDCl_3$, 500 MHz.

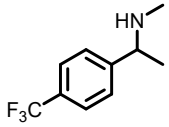

7a: Synthesized according to section **A.3.** ^{1}H NMR (500 MHz, $CDCl_3$): δ= 7.57 (d, J=8.1 Hz, 2H; Ar-H), 7.42 (d, J=7.9 Hz, 2H; Ar-H), 3.70 (q, J=6.7 Hz, 1H; CH), 2.29 (s, 3H; CH_3), 1.34 (d, J=6.6 Hz, 3H; CH_3). Solvent residual peaks: 5.29 (s, DCM), 1.58 (br s, water), 1.25 (br s, H grease)

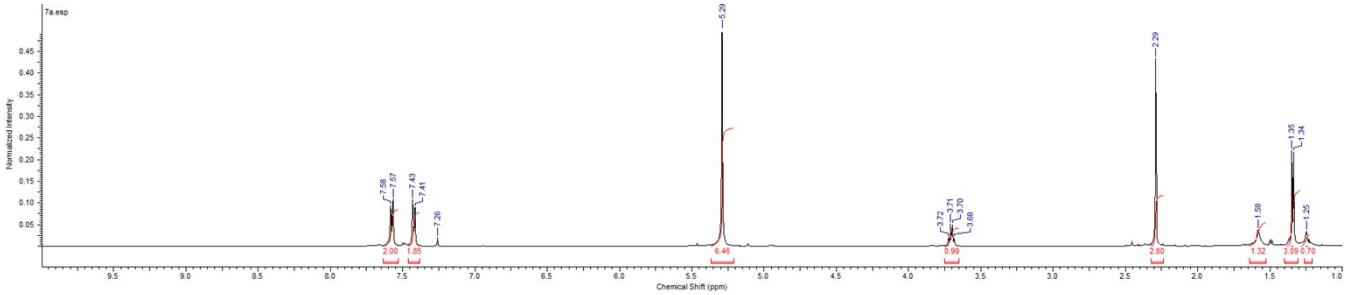

Figure S7. ^{1}H NMR spectrum of compound **7a** in $CDCl_3$, 500 MHz.

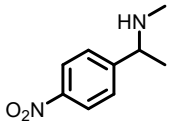

8a: Synthesized according to section **A.3.** ^{1}H NMR (500 MHz, $CDCl_3$): δ= 8.20-8.18 (m, 2H; Ar-H), 7.50-7.49(m, 2H; Ar-H), 3.77 (q, J=6.7 Hz, 1H; CH), 2.30 (s, 3H; CH_3), 1.35 (d, J=6.6 Hz, 3H; CH_3). Solvent residual peaks: 5.30 (s, DCM), 1.60 (br s, water), 1.25 (br s, H grease)

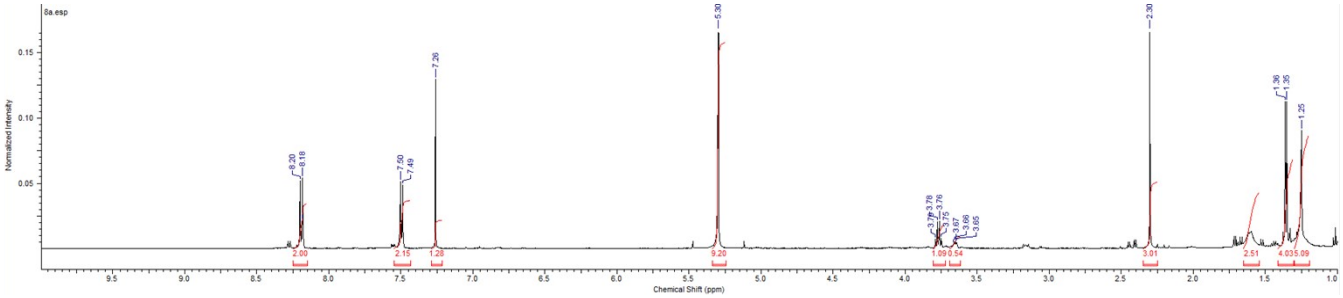

Figure S8. ^{1}H NMR spectrum of compound **8a** in $CDCl_3$, 500 MHz.

C.2. GC-MS

All the reaction products were analyzed by Gas chromatography-mass spectrometry (GC-MS) using Shimadzu Nexis GC-2030 coupled to Shimadzu GCMS-QP2020NX for identification and quantification unless mentioned. After each electrolysis ended, 2 µL of solution from the electrochemical cell was diluted with 998 µL of DCM. Then the 500-fold diluted solution was analyzed by GC-MS, both single-ion monitoring (SIM) and scan mode. External standard curves of amines obtained from commercial references or thermodynamically prepared samples of products using SIM mode in GCMSsolution Version 4.53SP1(Lab Solutions) software to quantify the product and derive the concentration of amines (C_{amine}) **(Section C.2.1)**. The partial current of amine (i_{amine}) values was calculated with the following equation:

i_{amine} = (Averaged total current) x (C_{amine} x n x F x V) / passed charge
Where n = 2, F = 96500 C/mol, V = 1.8 mL

To calculate the I_{amine} for the deuterated product, the same calibration curve was used for quantifying the deuterated amine based on the assumption that deuterium has a negligible effect on GCMS peak intensity.

C.2.1. GC-MS calibration curves for quantification

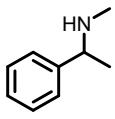

1a: commercially purchased chemical was used for the calibration curve. SIM analysis was conducted, m/z 120 ions detected at retention time 4.8 min was selected for the target ion, and m/z 58, 121 ions were selected for reference ions. The ratio of these ions in 1a was set for 100: 23.4 : 9.18 for m/z 120, 58, and 121 ions respectively based on NIST20-1,2 and NIST20s library in GCMS software. The allowance percentage was set at 70%.

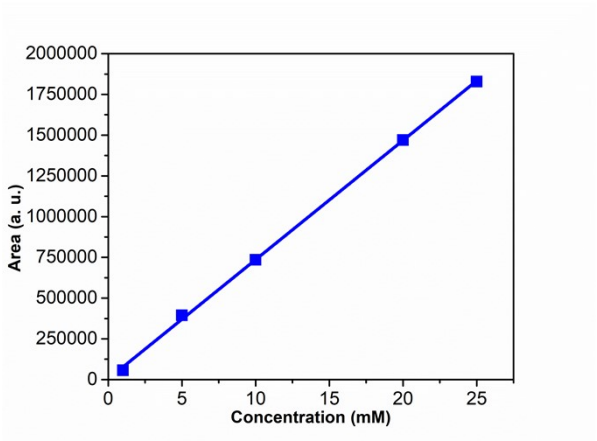

Figure S9. SIM calibration curve of compound **1a** (Slope: (7.32 ± 0.09) × 10^5, intercept: (0.39 ± 1.41) × 10^4, R-square value: 0.999)

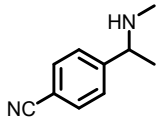

3a: Thermodynamically prepared sample was used for the calibration curve. SIM analysis was conducted, m/z 145.10 ion detected at retention time 7.3 was selected for target ion, and m/z 58.05, 146.05 ions were selected for reference ions. The ratio of these ions in 3a was set for 100: 25.3 : 20.6 for m/z 145.10, 58.05, 146.05 ions respectively. The allowance percentage was set at 70%.

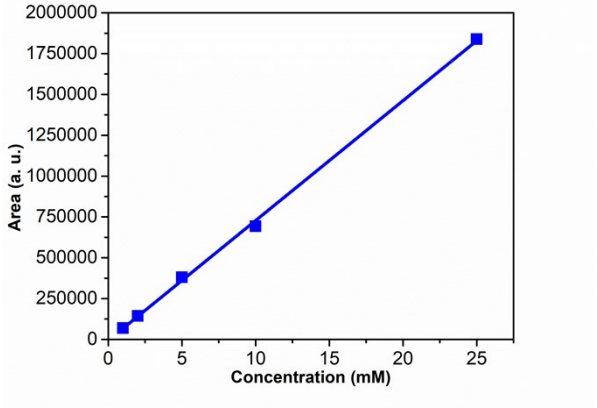

Figure S10. SIM calibration curve of compound **3a** (Slope: (7.34 ± 0.12) × 10^5, intercept: (-0.64 ± 1.48) × 10^4, R-square value: 0.999)

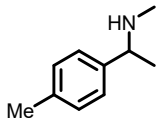

4a: Thermodynamically prepared sample was used for the calibration curve. SIM analysis was conducted, m/z 134.10 ion detected at retention time 5.7 was selected for target ion, and m/z 58.05, 91.10 ions were selected for reference ions. The ratio of these ions in 4a was set for 100: 20.1 : 17.0 for m/z 134.10: 58.05 : 91.10 ions respectively. The allowance percentage was set at 70%.

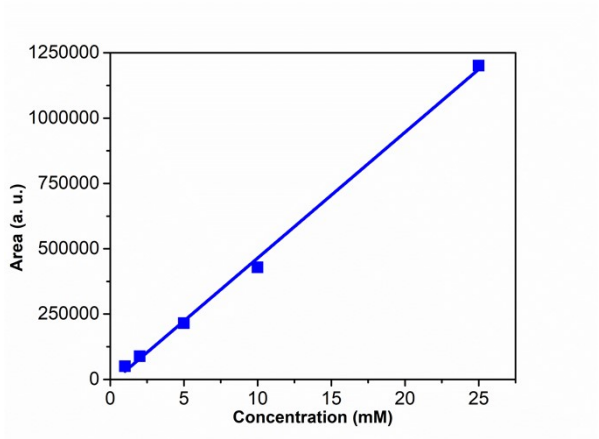

Figure S11. SIM calibration curve of compound **4a** (Slope: (4.82 ± 0.13) × 10^5, intercept: (-1.74 ± 1.61) × 10^5, R-square value: 0.997)

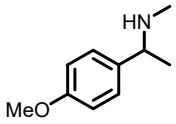

5a: Thermodynamically prepared sample was used for the calibration curve. SIM analysis was conducted, m/z 150.10 ion detected at retention time 6.8 was selected for target ion, and m/z 135.10, 58.05 ions were selected for reference ions. The ratio of these ions in **5a** was set for 100: 19.3 : 10.3 for m/z 150.10, 135.10, 58.05 ions respectively. The allowance percentage was set at 70%.

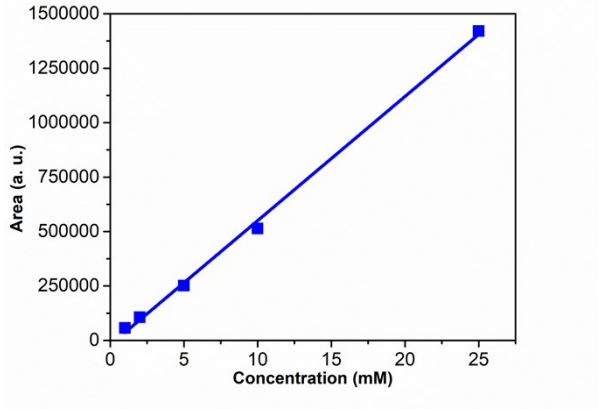

Figure S12. SIM calibration curve of compound **5a** (Slope: (5.70 ± 0.14) × 10^5, intercept: (-2.06 ± 1.72) × 10^5, R-square value: 0.998)

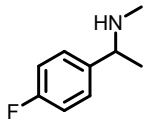

6a: Thermodynamically prepared sample was used for the calibration curve. SIM analysis was conducted, m/z 138.10 ion detected at retention time 4.9 was selected for target ion, and m/z 58.05, 103.05 ions were selected for reference ions. The ratio of these ions in 6a was set for 100: 16.2 : 14.7 for m/z 138.10, 58.05, and 103.05 ions respectively. The allowance percentage was set at 70%.

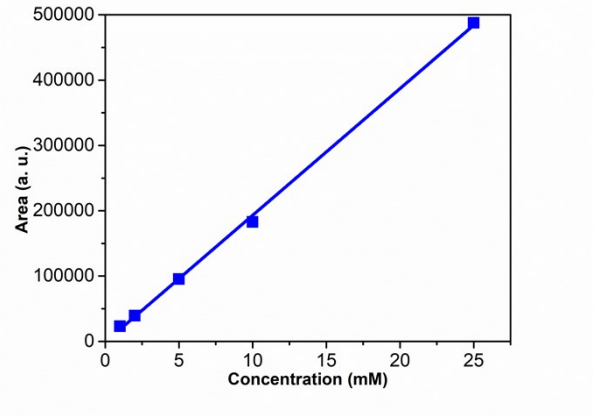

Figure S13. SIM calibration curve of compound **6a** (Slope: (1.94 ± 0.03) × 10^5, intercept: (-1.05 ± 4.28) × 10^4, R-square value: 0.999)

The SIM calibration curve of **7a** and **8a** was not obtained and used due to the failure of ERA using **7** and **8** respectively. (**Figure S20** and **S21**)

D. EPR spectroscopy

All EPR measurements were carried out at the Western Seoul center, Korea Basic Science Institute (KBSI) in Seoul, Korea. CW X-band (9.6 GHz) EPR spectra were collected on a Bruker EMX plus 6/1 spectrometer equipped with an Oxford Instrument ESR900 liquid He cryostat using an Oxford ITC 503 temperature controller. All spectra were collected with the following experimental parameters: microwave frequency, 9.6 GHz; microwave power, 0.3 mW; modulation amplitude, 10 G; time constant, 20.48 ms; 4 scans; temperature, 20 K.

Results and Discussion

E. Supplementary Figures

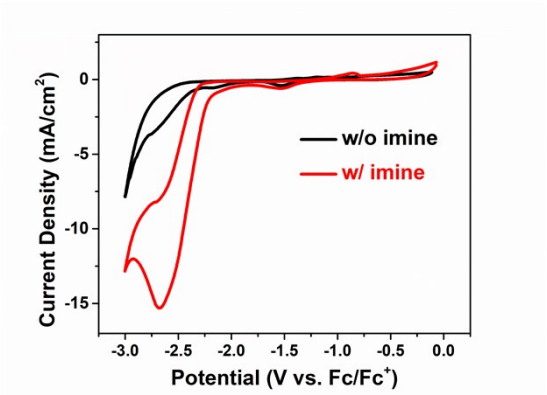

Figure S14. Cyclic voltammetry curves of with (red) and without (black) **1** (scan rate: 50 mV/s; 100 mM **1** was used)

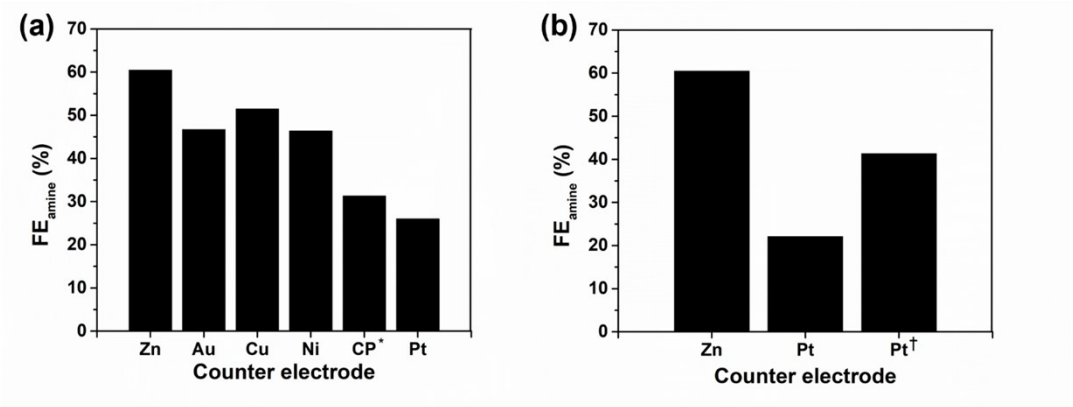

Figure S15 Effect of counter electrode materials. (a and b) Counter electrode dependence of FE_{amine}. *: CP is the abbreviation of carbon paper. † indicates the addition of Zinc acetate to the electrolyte solution. (electrolysis conditions: -2 mA, 8 C charge, DMSO with 300 mM of $^{n}Bu_4PF_6$ as electrolytes, 100 mM of **1**, and Cu as a working electrode).

Experiments with various counter electrode materials show that the Zn foil is the best candidate for a counter electrode in ERA among variance materials (**Figure S15a)**. While others (Au, Cu, and Ni) give similar FE_{amine}, Carbon paper, and Pt foil resulting in low FE_{amine} due to the oxidation of product amines [3]. Further, to investigate more about the Zn counter electrode system and determine whether the representative Lewis acid Zn^{2+} ions affect the FE_{amine}, an experiment is conducted by adding 23 mM of Zinc acetate (Zn^{2+} source, the concentration was calculated based on the assumption that all electrons come from the conversion of Zn to Zn^{2+}) **(Figure S15b)**. Zn^{2+} enhances the ERA, and a possible explanation is that Zn^{2+} interacts with nitrogen or in the imine moiety to make it more electrophilic, so that the rate-determining PCET step could be boosted. However, this effect is not significant because Zn and other metals (Au, Cu, and Ni) only have a little difference in FE_{amine}. In conclusion, Zn foil is selected for the counter electrode in optimized conditions because it works as a sacrificial anode to protect amine products from oxidation and Zn^{2+} might activate imine to additionally

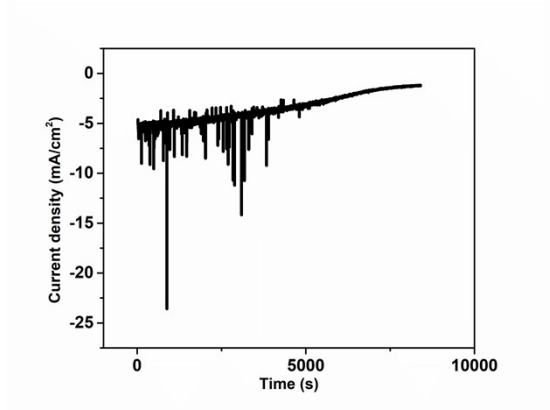

boost the ERA.

Figure S16. Current density graph when applied 2 F/mol at -2.86 V vs Fc/Fc^{+}. (Electrolysis condition: -2.86 V versus Fc/Fc+, 37.4 C passed, dimethyl sulfoxide (DMSO) with 300 mM $^{n}Bu_4PF_6$ as electrolytes, 100 mM **1**)

Current density decreased and showed a plateau over the reaction time and 80 % FE_{amine} was obtained after the reaction. The concentration of **1** decreased due to the ERA and GCMS confirmed that **1** was consumed thoroughly after the electrolysis. It led to the conclusion that the ERA requires two electrons and was comparable with our plausible reaction mechanism.

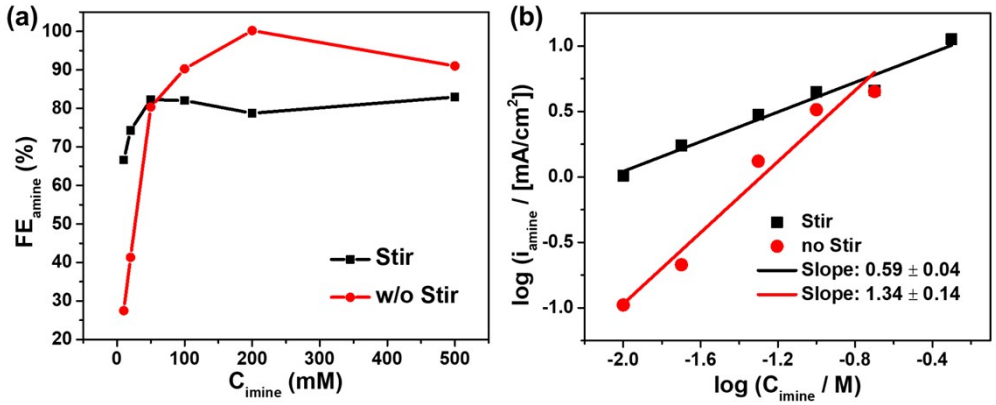

Figure S17. (a) FE_{amine} dependence on C_{imine} and (b) linear relationship between log (C_{imine}) and log ($|i_{amine}|$) at -2.86 V vs Fc/Fc+ with (black) and without (red) stirring. Electrolysis conditions: Cu/Zn electrodes, DMSO with 300 mM $^nBu_4PF_6$ as electrolytes, and 3 C (Black) or 5 C (Red) passed.

Vigorous stirring during the reaction resulted in the increased FE_{amine} when the C_{imine} was lower than 100 mM **(Figure S17a)**. Furthermore, the reaction order lessens from 1.34 to 0.57 in the presence of stirring **(Figure S17b)**. We assumed that stirring might help **1** to reach the electrode and accept the electrons at the low C_{imine} (<100 mM) conditions, however, at the higher C_{imine} conditions, cause the break of weak interaction through the electrode and desorption of **1** to inhibit the ERA. Thus, desorption can occur more easily to the point where the surface diffusion undergoes, which leads to the diffusion-controlled system and deviation of the reaction order from 1.

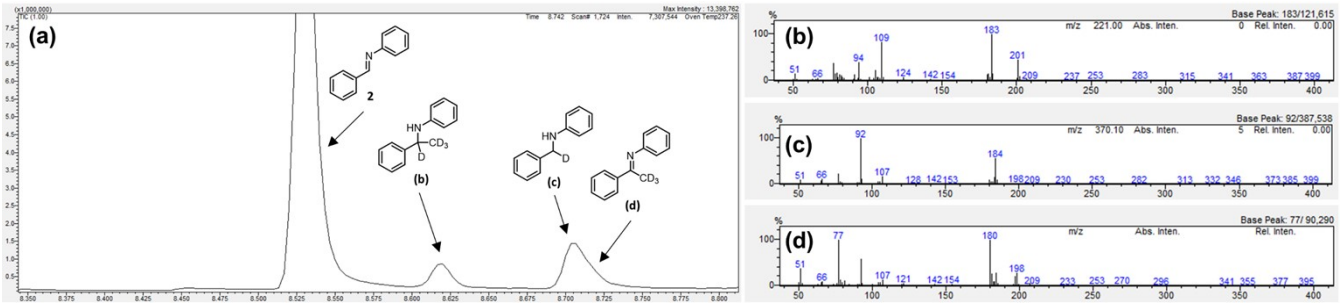

Figure S18. (a) GC-MS data resulted from the electrolysis of **2** at the DMSO-d6. Electrolysis condition: -1.65 mA/cm^2 chronopotentiometry analysis, 100 mM **2**, Cu/Zn electrodes, 300 mM $^nBu_4PF_6$ as electrolytes and 8 C passed. (b) MS (EI) m/z (%): 183.10 (100) [M-CD_3(18)]$^+$, 109.15 (87.25); tropylium ion with one deuterium and CD_3, 201.15 (43.75) [M]$^+$. (c) MS (EI) m/z (%): 92.10 (100) [M-92]$^+$;tropylium ion with one deuterium, 184.10 (56.30) [M]$^+$, 77.05 (22.75);benzene cation. (d) MS (EI) m/z (%): 77.05 (100); benzene cation, 180.10 (99.91) [M-CD_3(18)]$^+$, 198.15 (28.60) [M]+.

Electrolysis of **2** in DMSO-d_6 showed several deuterated products. Notably, the only ERA product that deuterium attached to benzylic carbon **(Figure S18c**, **2a**, α-deuterio-N-phenylbenzylamine**)** was observed while no hydrogenated product (**2a'**) was detected. Furthermore, methylated compounds **(Figure S18b, S18d)** were produced, and a detailed analysis of this phenomenon is now undergoing.

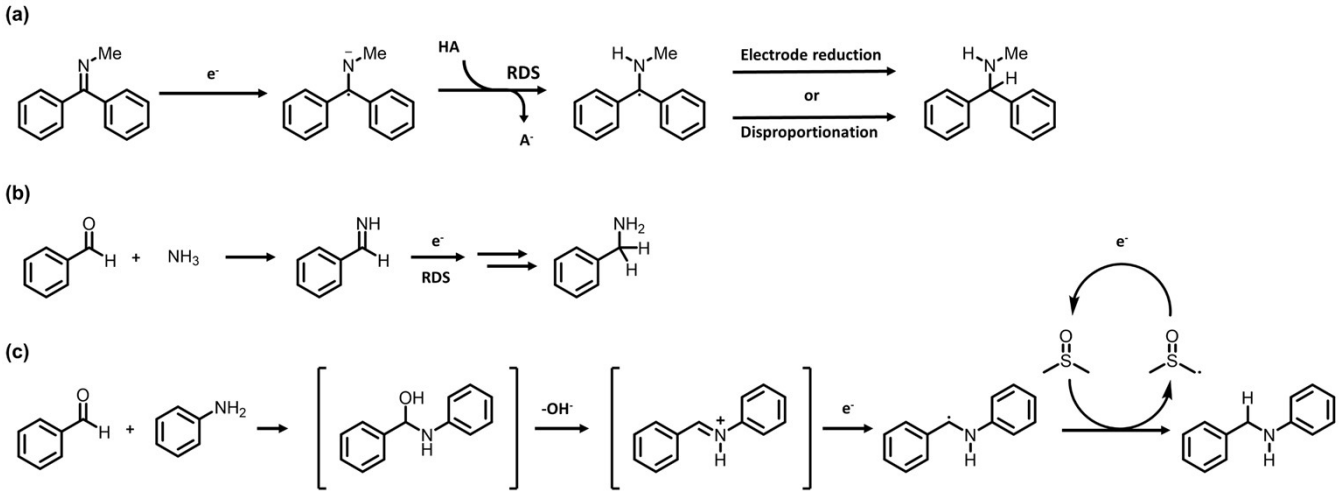

Figure S19. (a) Seveant group's[4], (b) Manthiram group's[5], and (c) Huang group's[6] reported ERA reaction mechanisms.

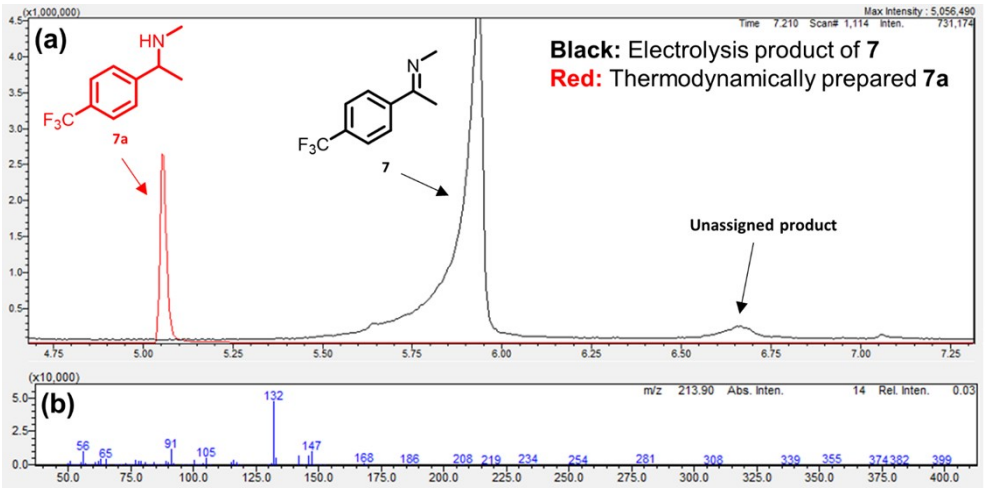

Figure S20. Failure of **7a** (R=CF_3). (a) Overlaid GCMS data of electrolysis product of **7** (**black**) and thermodynamically prepared **7a** (**Red**). (b) MS fragmentation pattern of unassigned product in (a). The top 5 highest intensity ions; m/z (%): 132.10 (100), 91.10 (26.23), 56.05 (22.82), 147.10 (22.45), 146.10 (15.76).

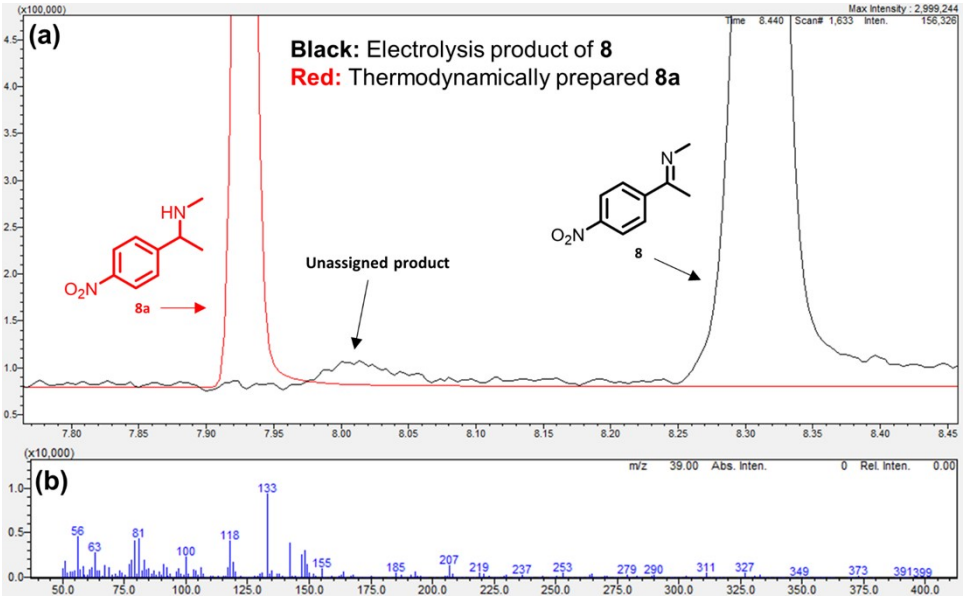

Figure S21. Failure of **8a** (R=NO_2). (a) Overlaid GCMS data of 8 (black) electrolysis products and thermodynamically prepared **8a** (**Red**). (b) MS fragmentation pattern of unassigned product in (a). The top 5 highest intensity ions; m/z (%): 133.10 (100), 56.05 (49.56), 81.05 (47.52), 79.00 (44.97), 118.05 (44.43).

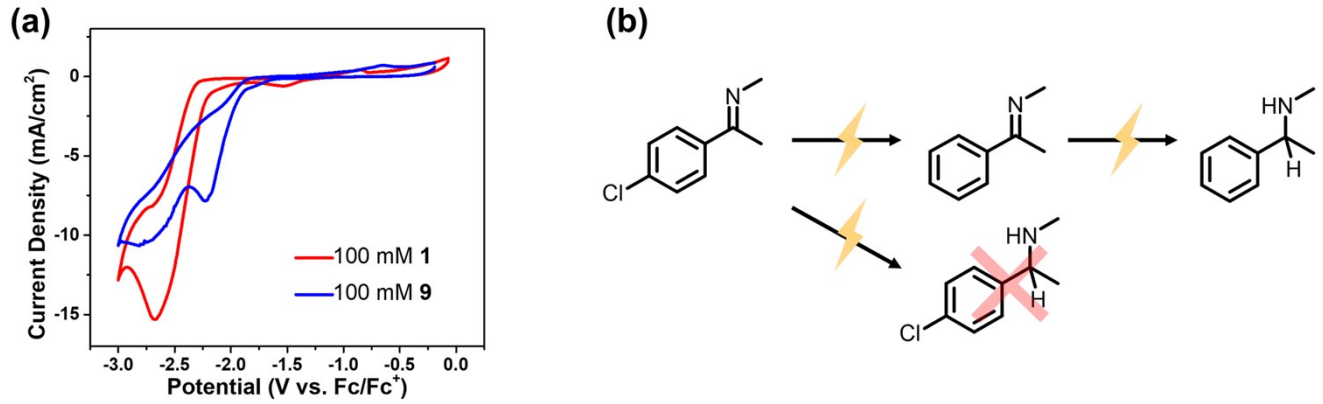

Figure S22. (a) Cyclic voltammetry curves of 100 mM **1** (red) and **9** (blue) (scan rate: 50 mV/s; 100 mM substrate). (b) Observed electrolysis pathway of **9**.

7,8 and **9** were selected as a substrate for the Hammett plot due to the presence of the various functional groups (trifluoromethyl, nitro, and chlorine group) which act as an electron-withdrawing group. However, GC-MS analysis of an electrolyzed product revealed that their fragmentation pattern was not matched with the thermodynamically synthesized reductive amination products for **7** and **8** **(Figure S20** and **S21)**. Also, dechlorination occurred before the ERA proceeded in the case of using **9** as a substrate **(Figure S22)**. Further electrolysis resulted in **1a** with a lower FE_{amine} compared to the start with **1** as substrate.

Author Contributions

Conceptualization: T. K., D. I. P., H. J. Y., and K. J.; Supervision: H. J. Y., and K. J.; Validation: T. K., and S. K.; Investigation: T. K., D. I. P., S. K., D. Y., S. H., S. H. K., and K. J.; Visualization: T. K., and K. J.; Writing-original draft: T. K., and K. J.; Writing-review & editing: T. K., D. I. P., D. Y., S. H., S. H. K., H. J. Y., and K. J.; Project administration: T. K., H. J. Y., K. J.

Reference

[1] C. K. Blasius, N. F. Heinrich, V. Vasilenko, L. H. Gade, Angewandte Chemie - International Edition **2020**, 59, 15974–15977.

[2] G. R. Fulmer, A. J. M. Miller, N. H. Sherden, H. E. Gottlieb, A. Nudelman, B. M. Stoltz, J. E. Bercaw, K. I. Goldberg, Organometallics **2010**, 29, 2176–2179.

[3] A. Adenier, M. M. Chehimi, I. Gallardo, J. Pinson and N. Vilà, Langmuir, 2004, **20**, 8243–8253.

[4] C. P. Andrieux, J. M. Saveant, J. Electroanal. Chem. **1971**, 33, 453–461.

[5] Z. J. Schiffer, M. Chung, K. Steinberg, K. Manthiram, Chem Catalysis, **2023**, 100500.

[6] H. Hong, Z. Zou, G. Liang, S. Pu, J. Hu, L. Chen, Z. Zhu, Y. Li, Y. Huang, Org Biomol Chem **2020**, 18, 5832–5837.